Supplement of Geosci. Model Dev., 17, 3487–3505, 2024
https://doi.org/10.5194/gmd-17-3487-2024-supplement

Geoscientific Model Development
Open Access
EGU

Supplement of

Assessing acetone for the GISS ModelE2.1 Earth system model

Alexandra Rivera et al.

Correspondence to: Kostas Tsigaridis (kostas.tsigaridis@columbia.edu)

Chemical sources

The acetone molar yields of propane, butane, pentane, and higher alkanes were derived with suggestions from the literature (Fischbeck et al., 2017; Jacob et al., 2002; Weimer et al., 2017). We used a molar yield of 0.73 for propane, derived by averaging 0.72 from Jacob et al. (2002) and 0.736 from Weimer et al. (2017). Our molar yield of 0.95 for butane was derived by averaging 0.96 from Fischbeck et al. (2017) and 0.93 from Jacob et al. (2002). Our molar yield of 0.63 for pentane was derived by averaging 0.72 from Fischbeck et al. (2017) and 0.53 from Jacob et al. (2002). Finally, we used a molar yield of 0.79 for higher alkanes, derived from averaging the following four values: 0.96 for isobutane and 0.72 for isopentane in Fischbeck et al. (2017), and 0.93 for isobutane and 0.53 for isopentane in Jacob et al. (2002).

Global acetone budget and burden

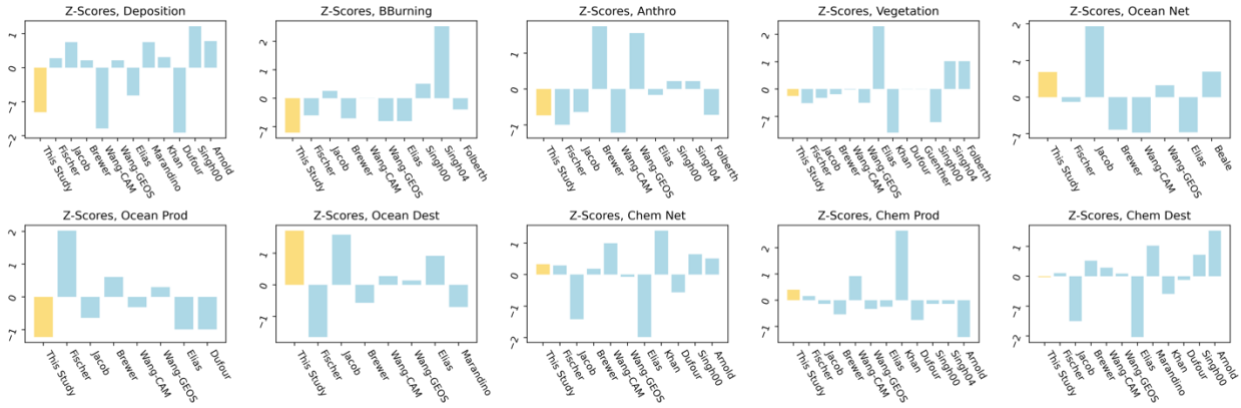

Figure S1. The data recorded in the literature was used to determine a mean for each budget flux value, and the distance from that mean for each paper was expressed as a *z*-score (Arnold et al., 2005; Beale et al., 2013; Brewer et al., 2017; Dufour et al., 2016; Elias et al., 2011; Fischer et al., 2012; Folberth et al., 2006; Guenther et al., 2012; Jacob et al., 2002; Khan et al., 2015; Marandino et al., 2006; Singh et al., 2000, 2004; Wang et al., 2020).The *z*-scores for the literature are in shown as light-blue bars, and the Baseline model's *z*-score is highlighted in yellow.

Spatial distribution of acetone

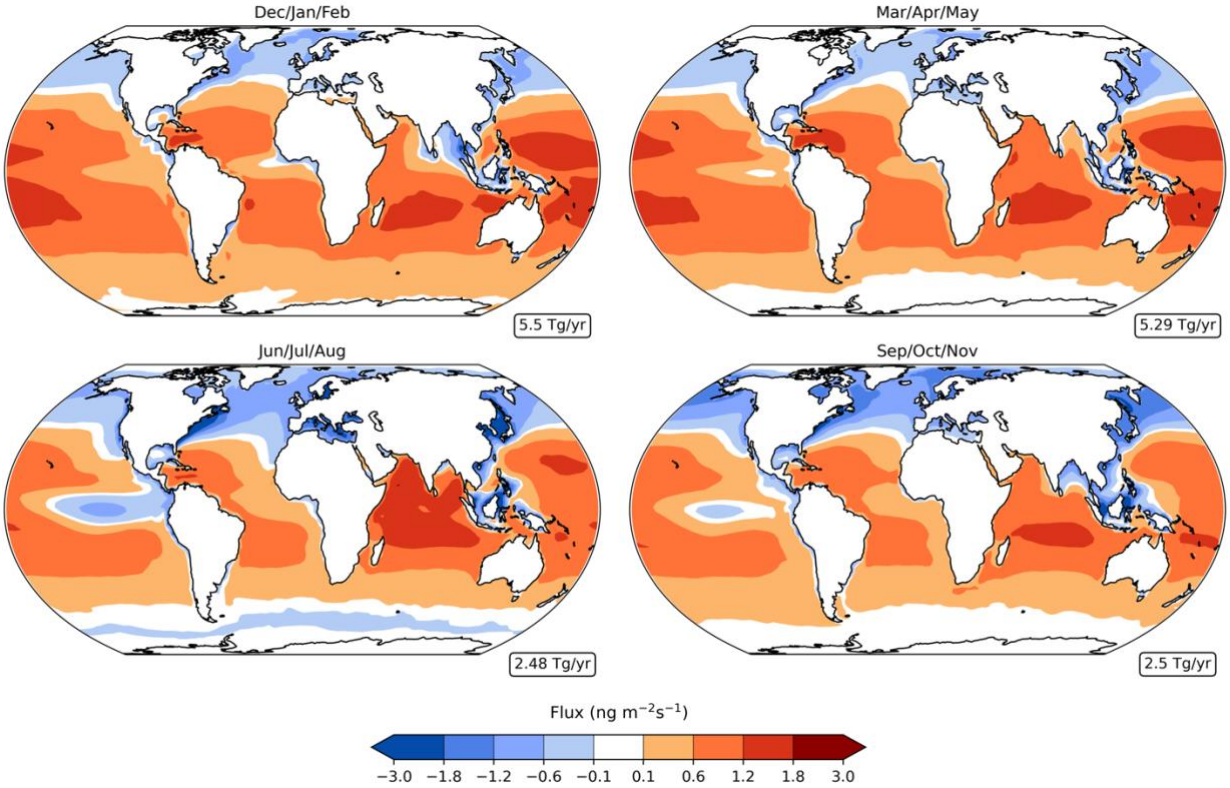

Figure S2. Net oceanic acetone fluxes in the Baseline simulation for December-February (top left), March-May (top right), June-August (bottom left), and September-November (bottom right), with red indicating a net source and blue indicating a net sink. Nonlinear colorbars are used to better differentiate the details in the map. The weighted global means of the net ocean fluxes are shown in boxes on the lower right of each subplot.

Vertical distribution of acetone

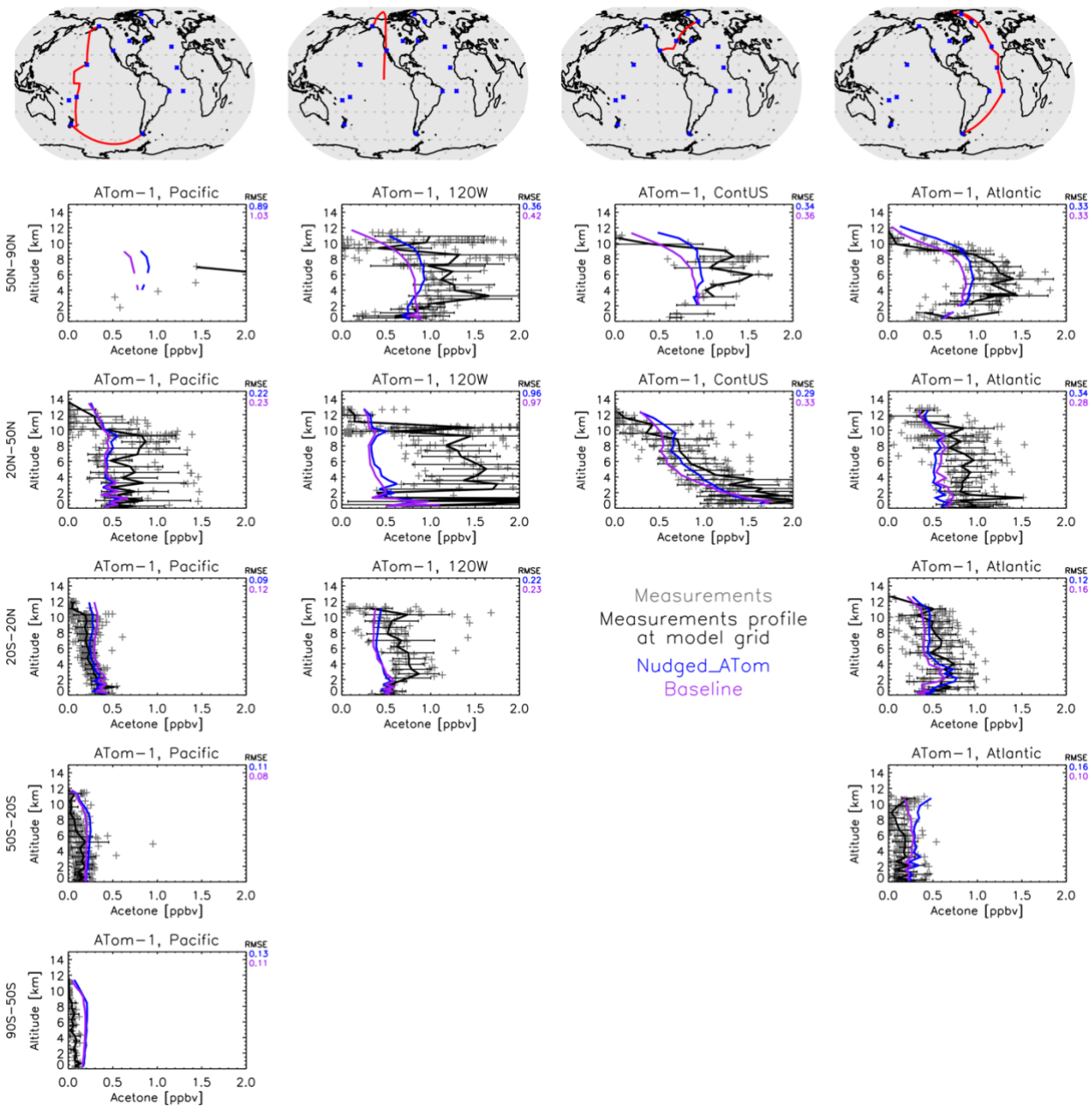

Figure S3. Comparison between the GISS ModelE2.1 simulations (Baseline in purple and Nudged_ATom in blue) and the ATom-1 field measurements (July-August 2016). Individual data points are shown with dark grey symbols, and their average values are shown in black, with error bars representing the one-sigma range of the averages. The root mean square error (RMSE) of each simulation is noted at the top right of each subplot.

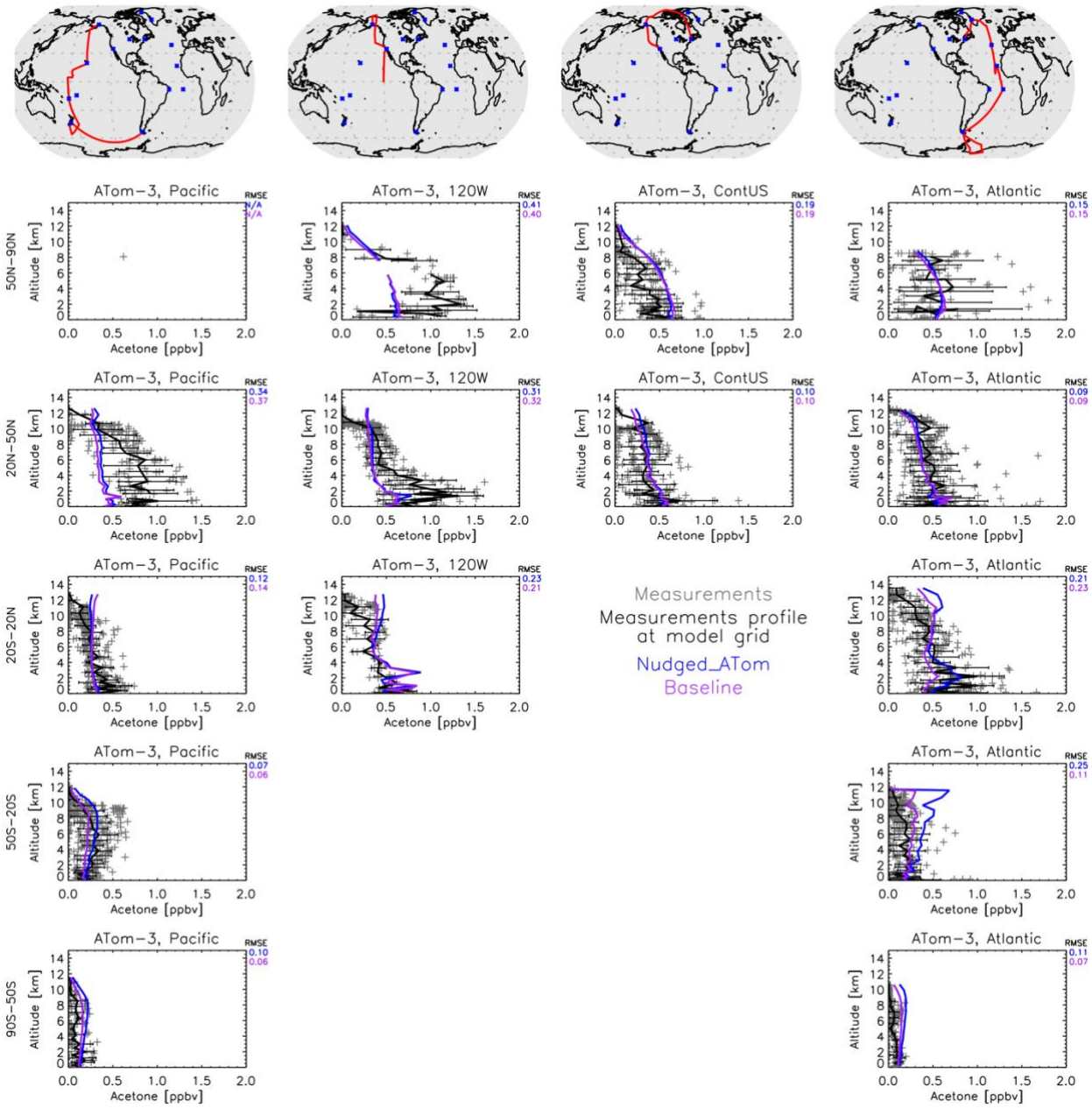

Figure S4. Similar to Figure S3, except for the ATom-3 field measurements (September-October 2017).

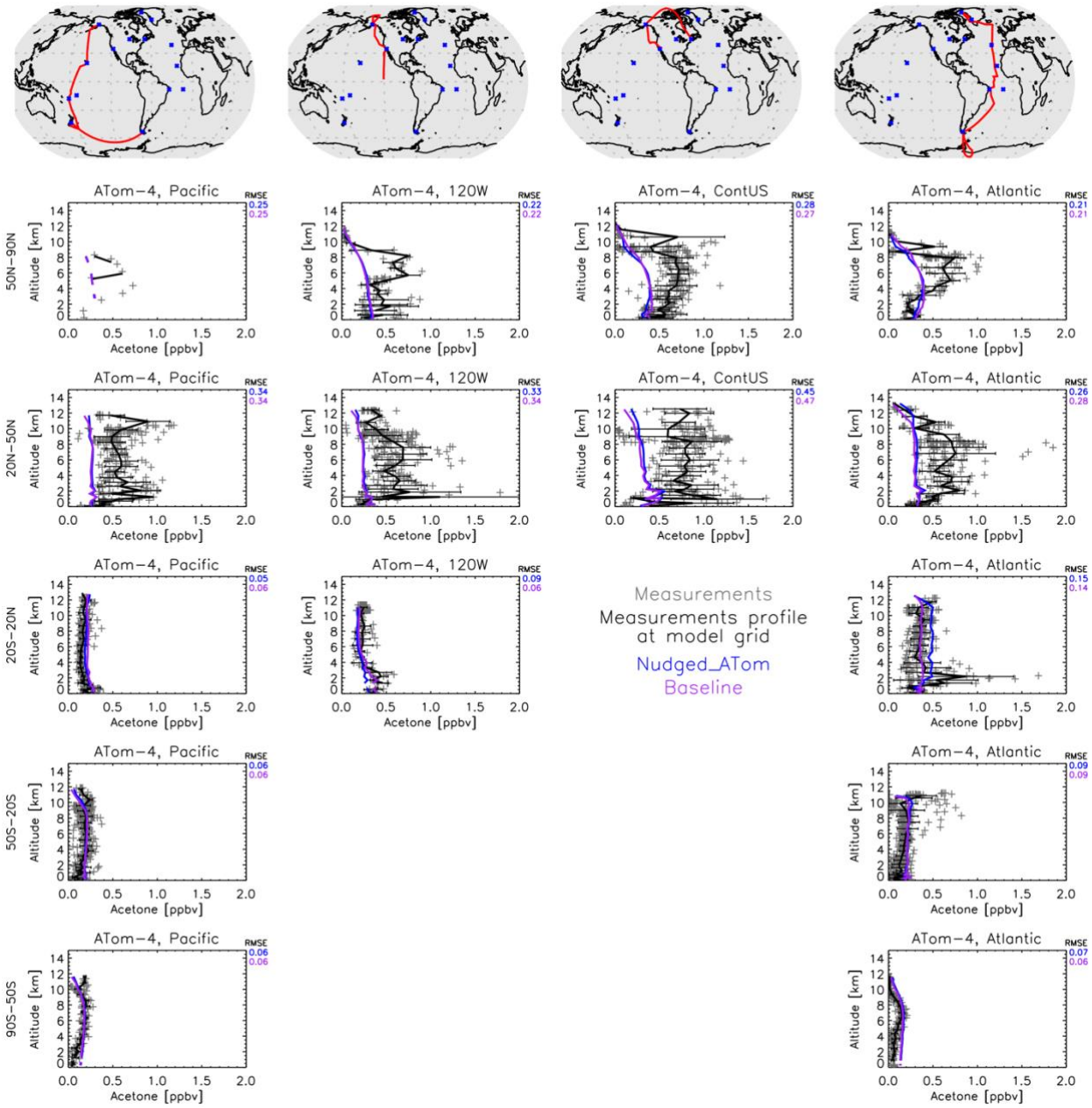

Figure S5. Similar to Figure S3, except for the ATom-4 field measurements (April-May 2018).

Seasonality of acetone

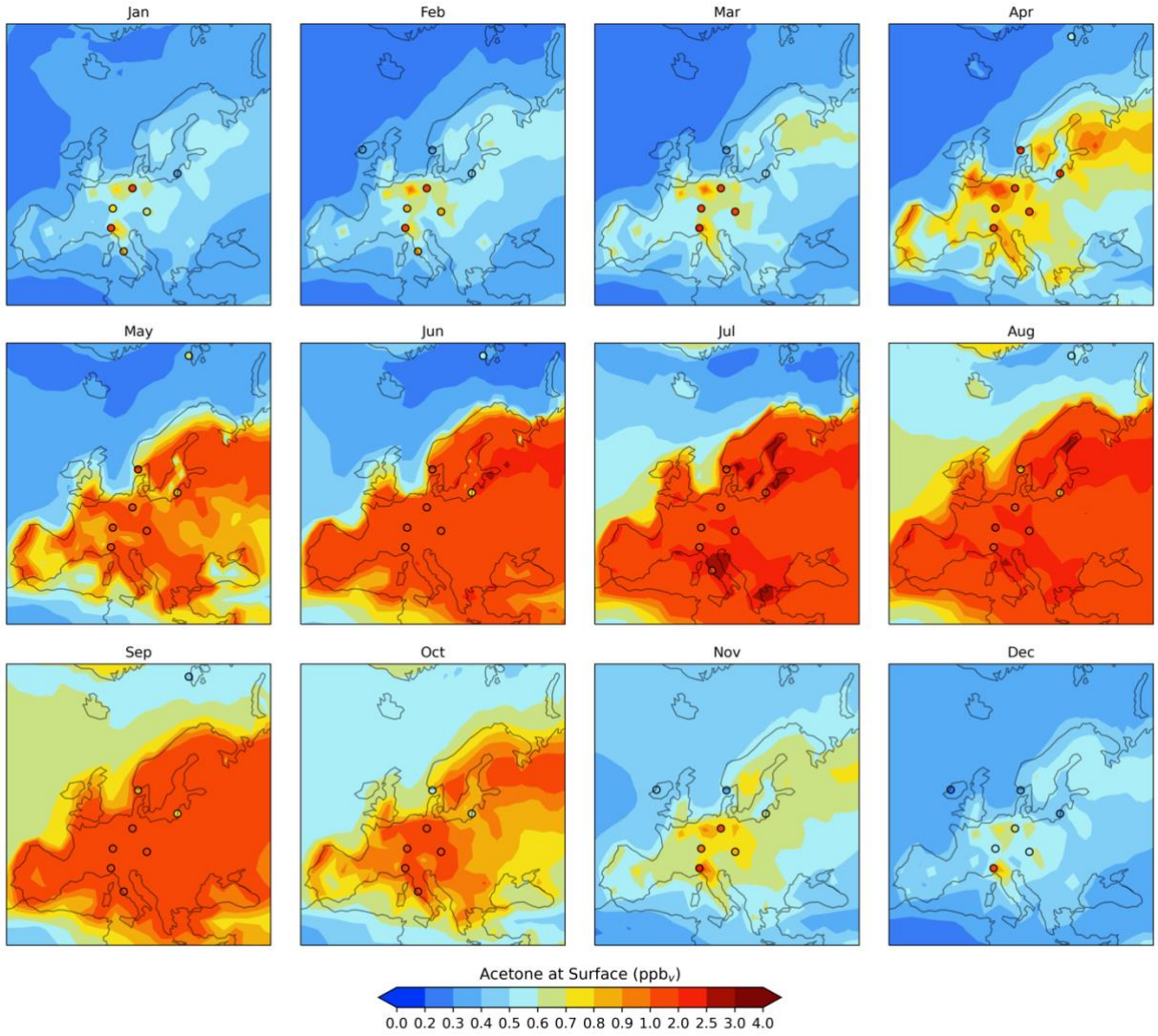

Figure S6. GISS ModelE2.1 spatial distribution of annual mean acetone at surface for the Baseline simulation in Europe over twelve months. Filled circles represent data from field measurements from Solberg et al. (1996). A nonlinear colorbar is used to better differentiate the details in the map.

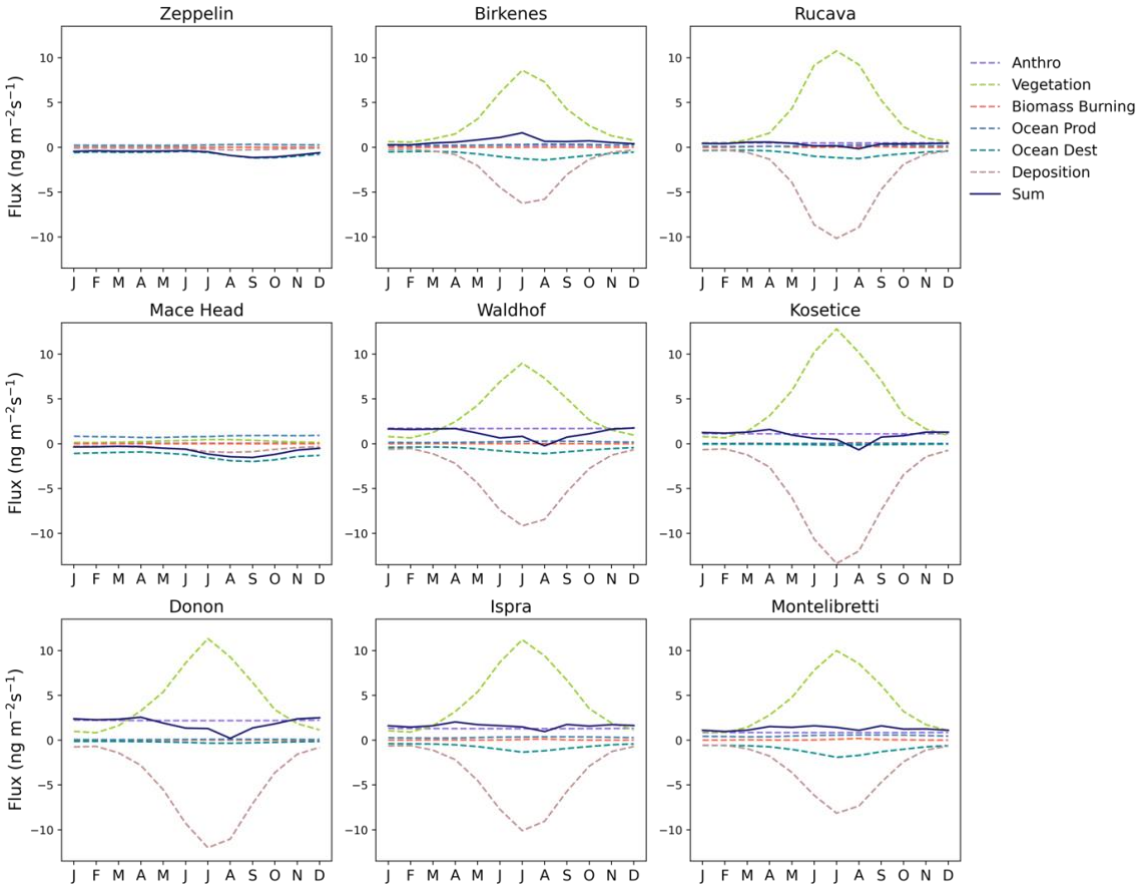

Figure S7. Contribution of acetone sources and sinks in the Baseline simulation over twelve months on the regional level (10˚ x 12.5˚ grid boxes) at nine European sites. The sources and sinks are shown as various colored dashed lines, and their sums are shown as solid navy-blue lines.

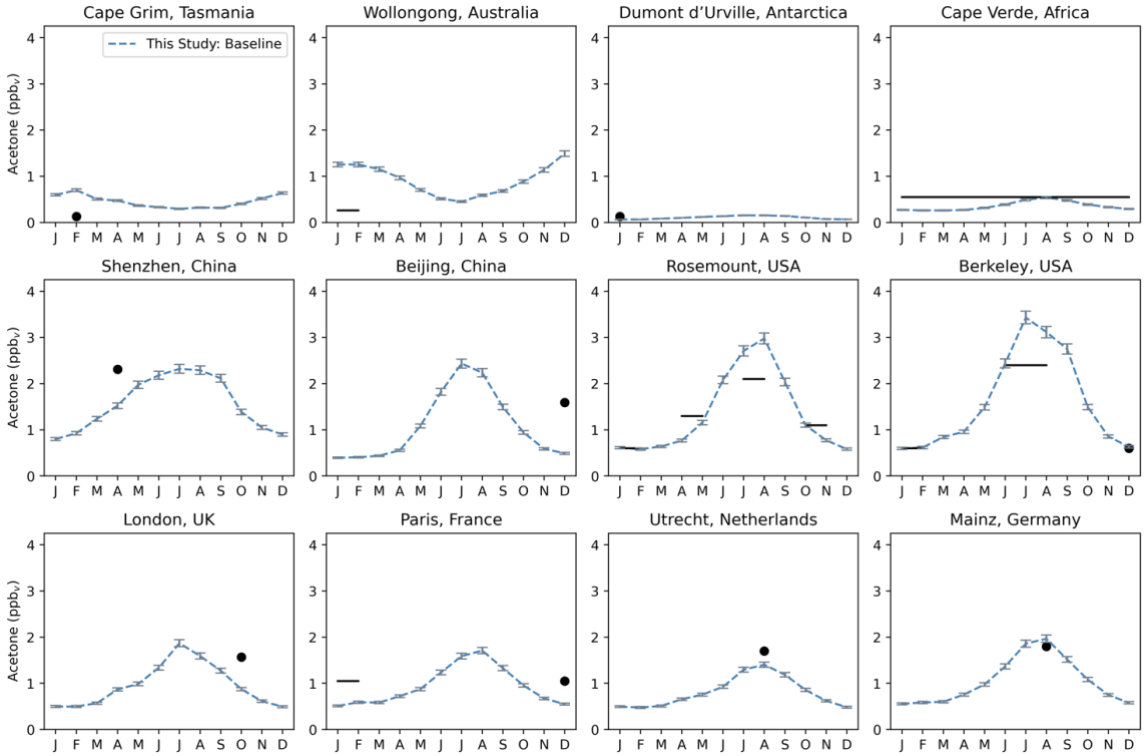

Figure S8. Acetone over twelve months for various sites that do not have enough measurements to resolve seasonality (Australia, Antarctica, Africa, Asia, Europe, North America). The modeled estimates of acetone at the surface from the Baseline simulation are shown as dashed blue lines and the grey error bars represent the one-sigma range of the modeled concentrations in the climatological mean of 5 years. The modeled estimates are overlaid with monthly (solid circles) or seasonal (solid lines) field measurements, as found in the literature (de Gouw et al., 2004; Dolgorouky et al., 2012; Galbally et al., 2007; Guérette et al., 2019; Hu et al., 2013; Huang et al., 2020; Langford et al., 2010; Legrand et al., 2012; Li et al., 2019; Read et al., 2012; Schade and Goldstein, 2006).

Sensitivity Studies

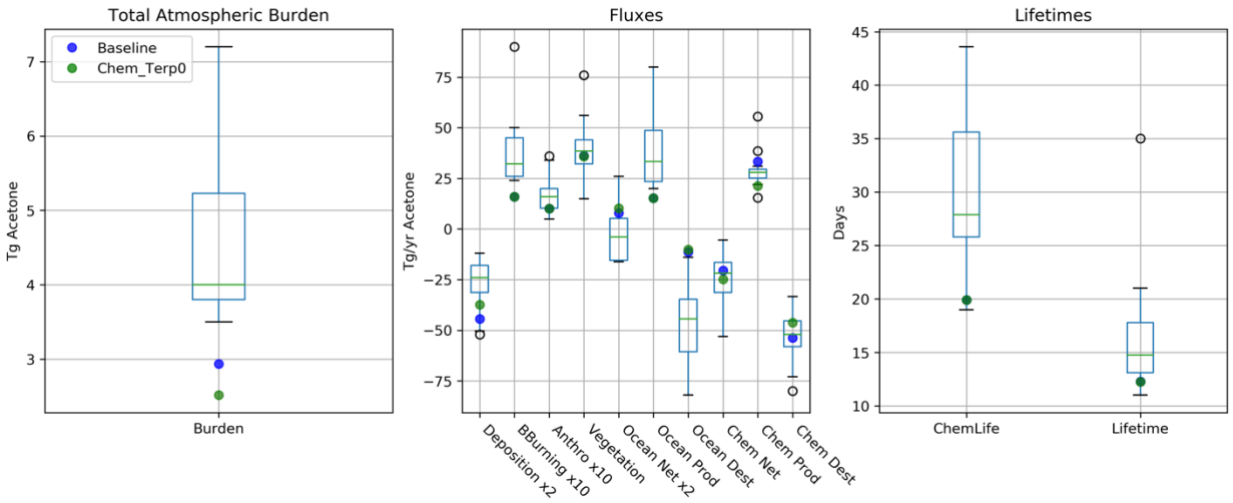

Figure S9. Total atmospheric burden, fluxes, and lifetimes of acetone from the literature (shown in boxes and whiskers with outliers as open circles) (Arnold et al., 2005; Beale et al., 2013; Brewer et al., 2017; Dufour et al., 2016; Elias et al., 2011; Fischer et al., 2012; Folberth et al., 2006; Guenther et al., 2012; Jacob et al., 2002; Khan et al., 2015; Marandino et al., 2006; Singh et al., 2000, 2004; Wang et al., 2020), values from GISS ModelE2.1 Baseline simulation (solid blue circles), and values from the Chem_Terp0 sensitivity study (green circles).

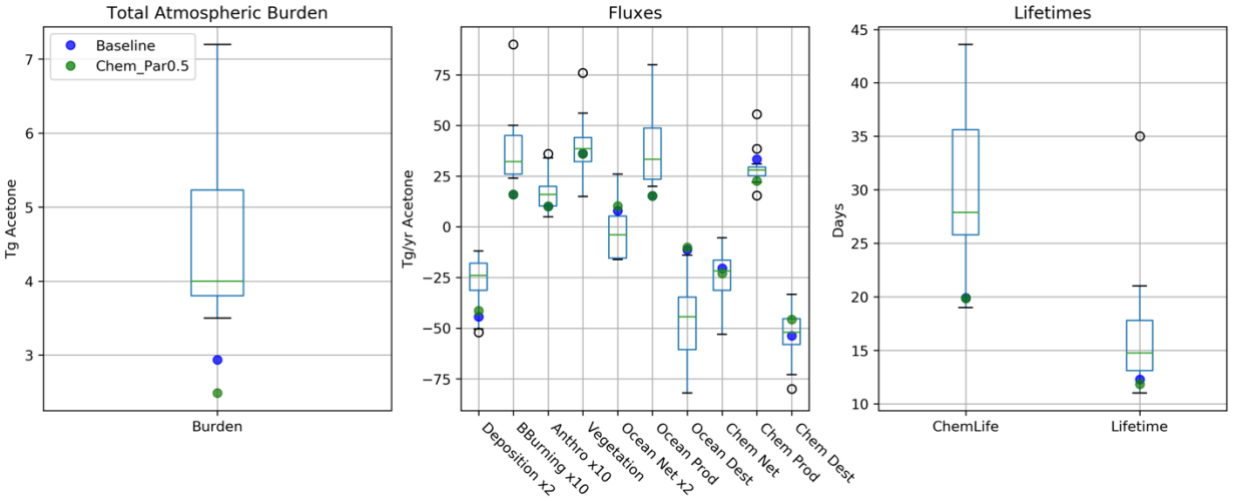

Figure S10. Similar to Figure S9, except values from the Chem_Par0.5 sensitivity study as green circles.

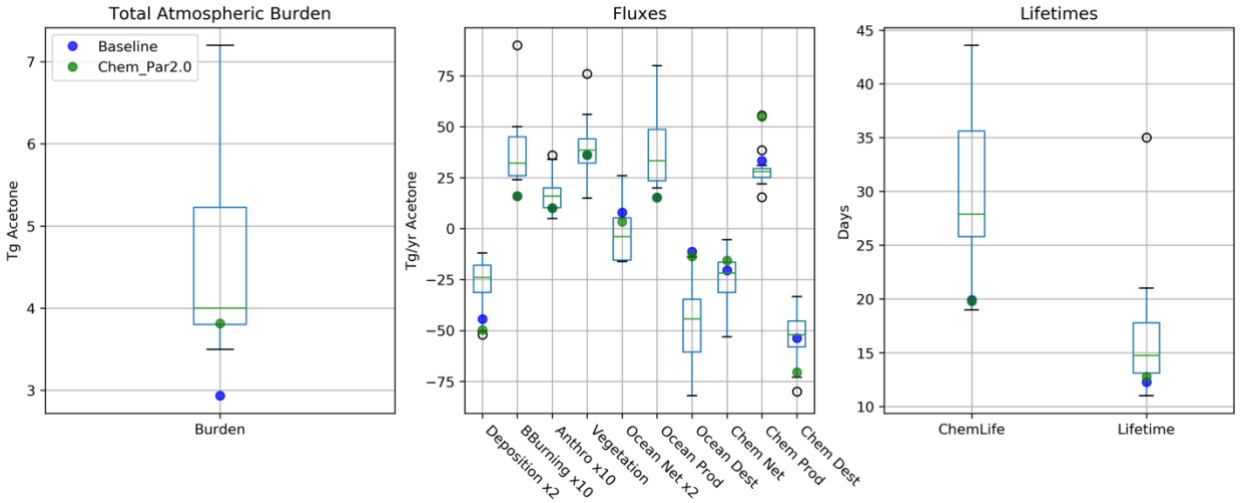

Figure S11. Similar to Figure S9, except values from the Chem_Par2.0 sensitivity study as green circles.

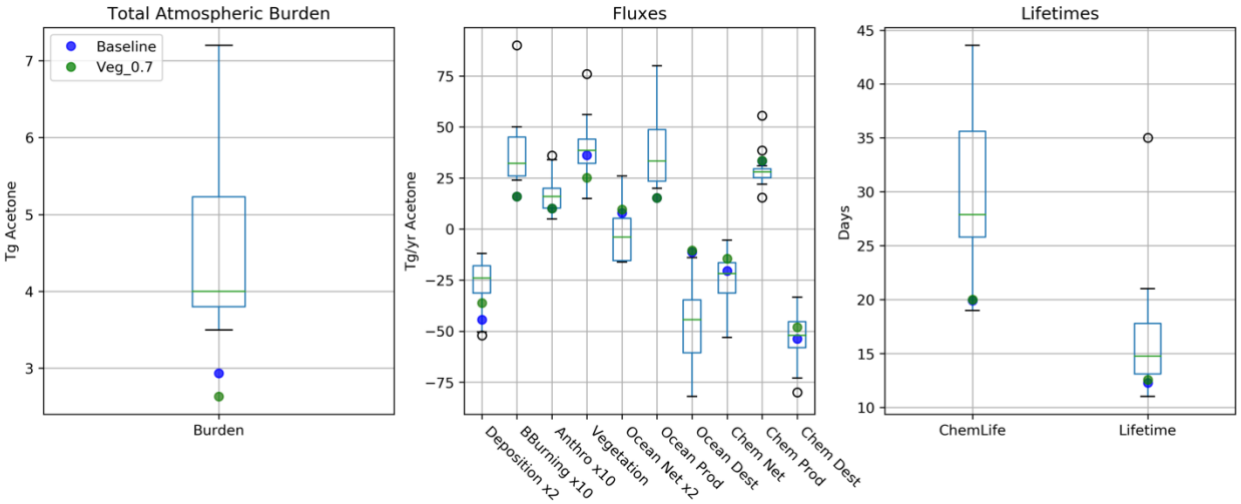

Figure S12. Similar to Figure S9, except values from the Veg_0.7 sensitivity study as green circles.

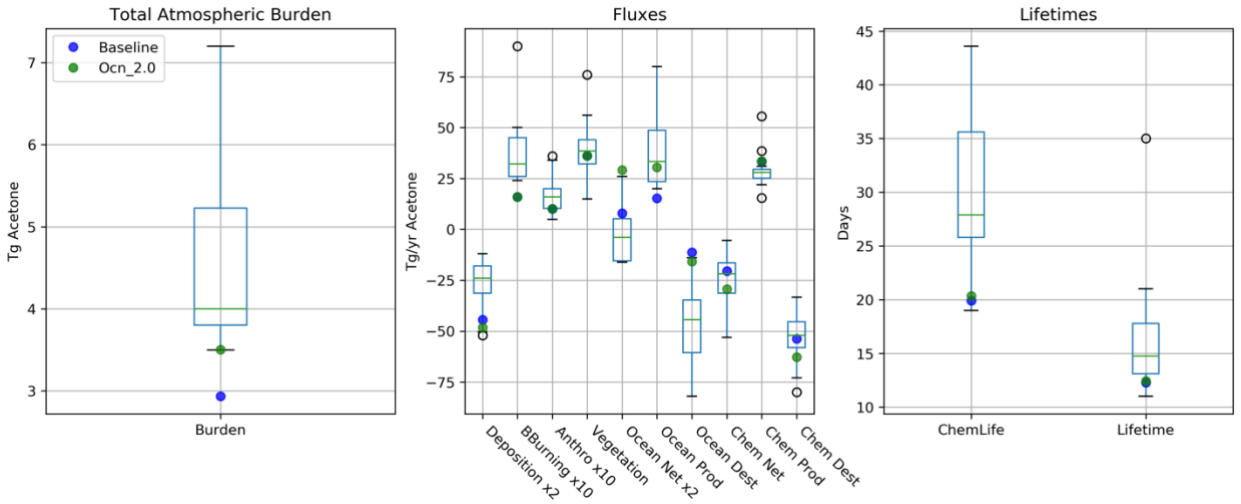

Figure S13. Similar to Figure S9, except values from the Ocn_2.0 sensitivity study as green circles.

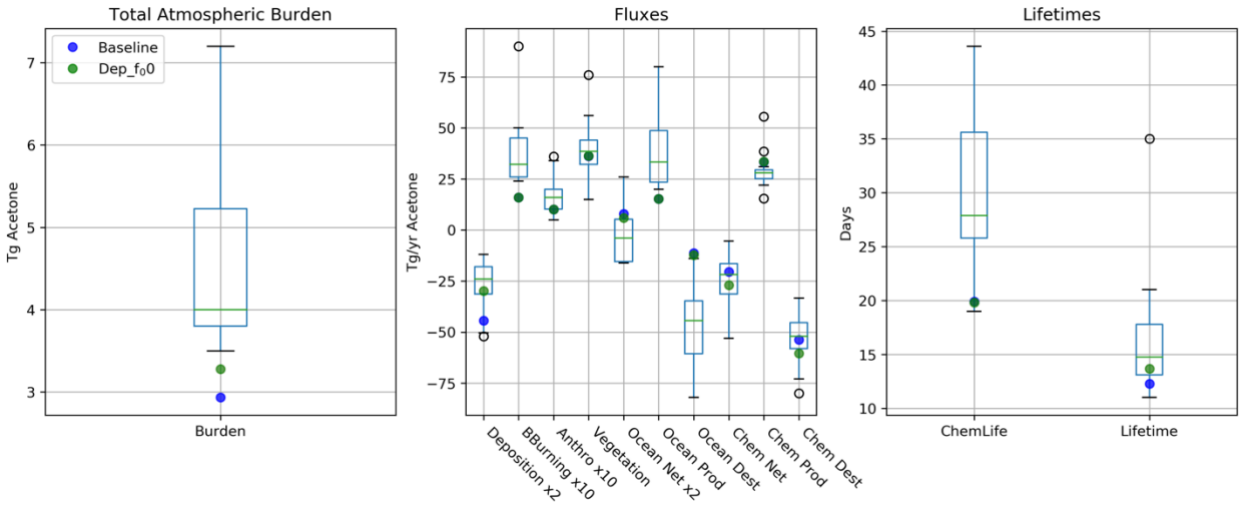

Figure S14. Similar to Figure S9, except values from the Dep_f$_0$0 sensitivity study as green circles.

Chemistry

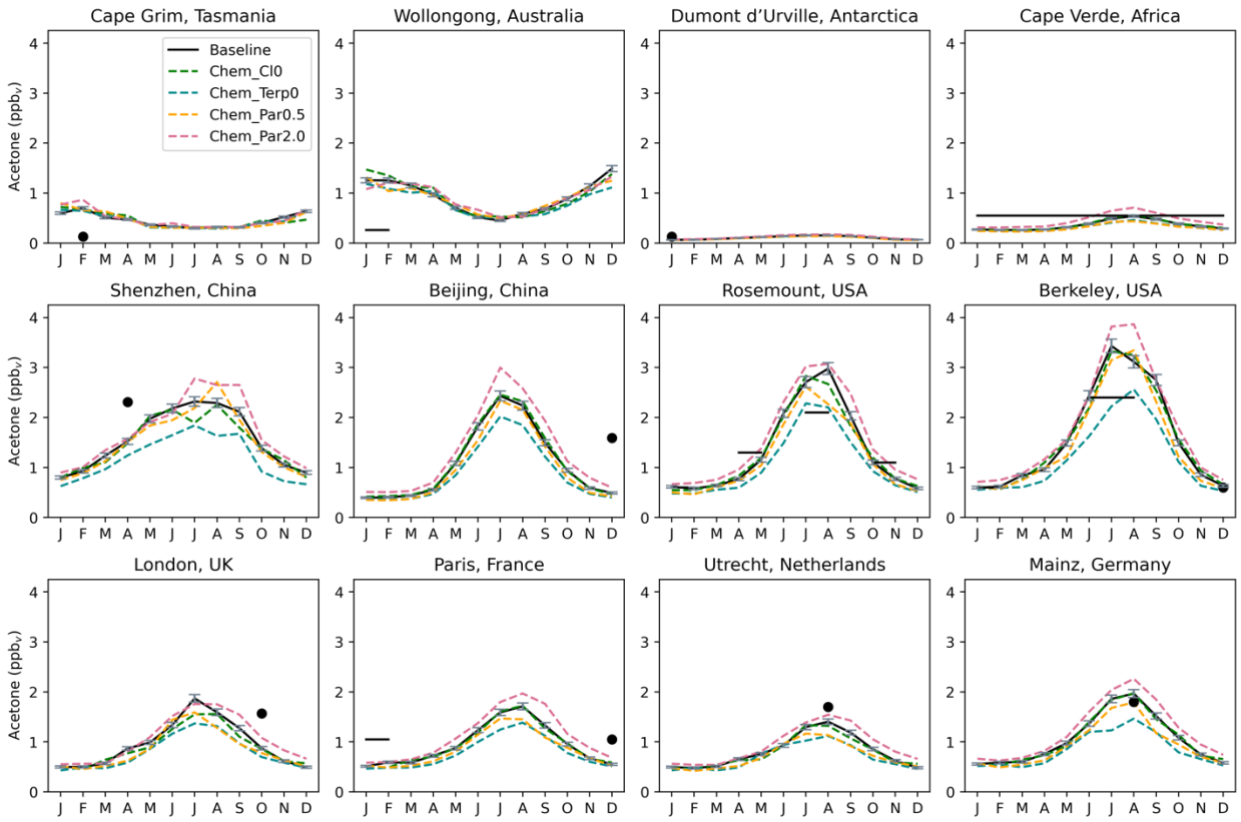

Figure S15. Similar to Figure S8, but with the chemistry sensitivity studies added. The modeled estimates of acetone at the surface from the Baseline simulation are shown as solid black lines, and the sensitivity studies are as follows: removing the acetone + chlorine reaction (dashed green lines), removing the production of acetone from terpenes (dashed blue lines), halving the yield of acetone from paraffin (dashed orange lines), and doubling the yield of acetone from paraffin (dashed pink lines). The modeled estimates are overlaid with monthly (solid circles) or seasonal (solid lines) field measurements, as found in the literature (de Gouw et al., 2004; Dolgorouky et al., 2012; Galbally et al., 2007; Guérette et al., 2019; Hu et al., 2013; Huang et al., 2020; Langford et al., 2010; Legrand et al., 2012; Li et al., 2019; Read et al., 2012; Schade and Goldstein, 2006).

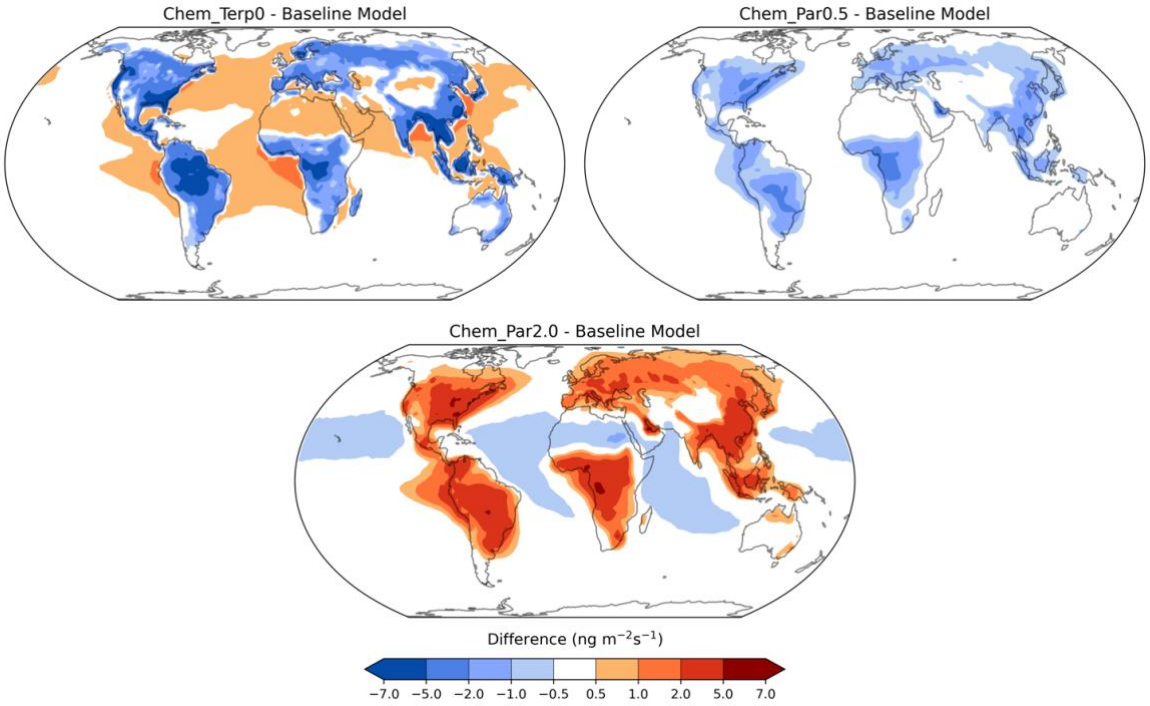

Figure S16. Chemistry sensitivities anomalies from Baseline, with red indicating an increase and blue indicating a decrease of the column-integrated net acetone chemistry flux. Nonlinear colorbars are used to better differentiate the details in the map. The fourth chemistry sensitivity study, Chem_Cl0, is omitted as the anomalies from Baseline are negligible.

Terrestrial and oceanic fluxes

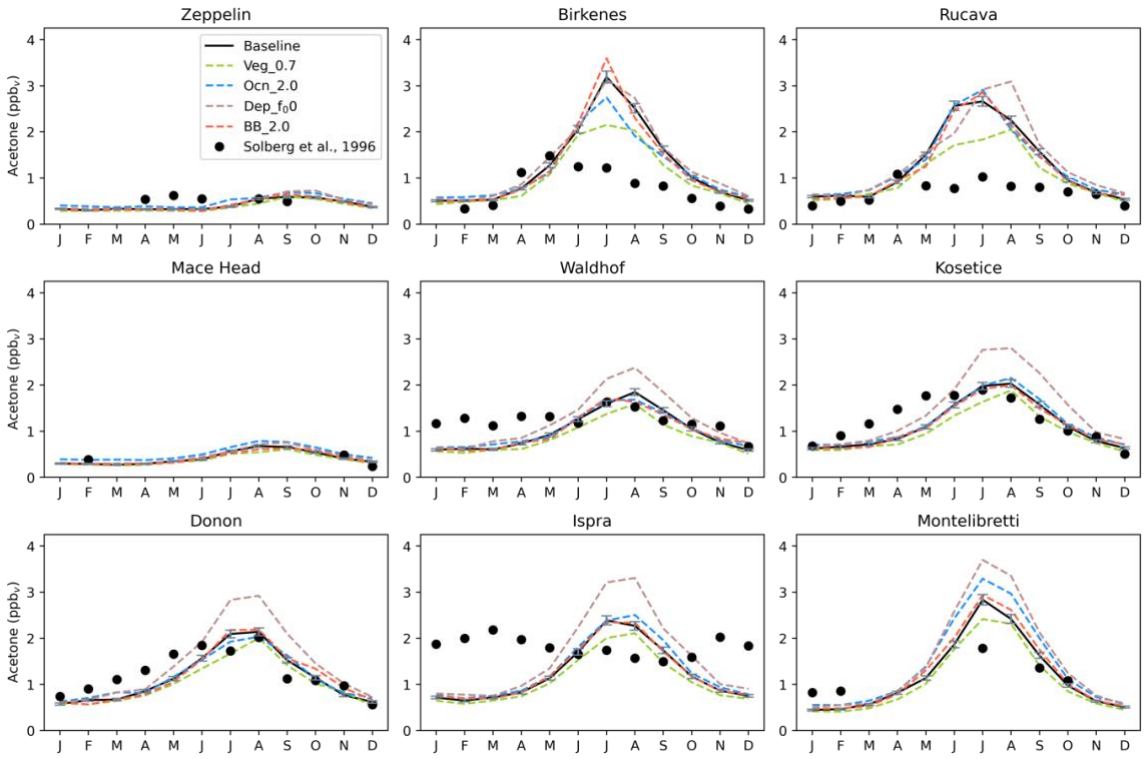

Figure S17. Acetone over twelve months at nine European sites with the terrestrial and oceanic sensitivity studies added. The modeled estimates of acetone at the surface from the Baseline simulation are shown as solid black lines, and the sensitivity studies are as follows: reducing vegetation emissions to 0.7 acetone from MEGAN (dashed light-green line), doubling ocean acetone concentration (dashed blue line), changing the reactivity factor for dry deposition (dashed brown line), and doubling biomass burning emissions (dashed orange line). Field measurements from Solberg et al., (1996) are shown as solid black dots.

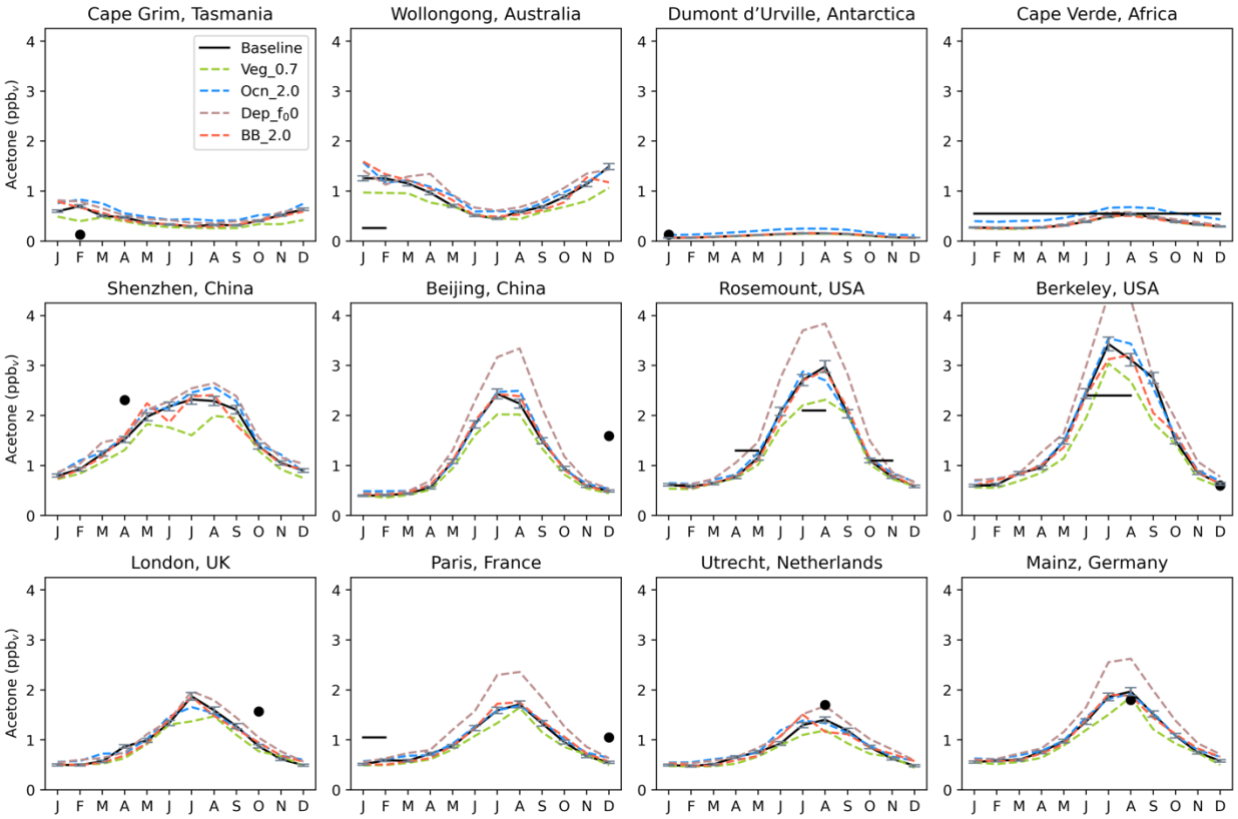

Figure S18. Similar to Figure S8, but with the terrestrial and oceanic sensitivity studies added. The modeled estimates of acetone at the surface from the Baseline simulation are shown as solid black lines, and the sensitivity studies are as follows: reducing vegetation emissions to 0.7 acetone from MEGAN (dashed light-green line), doubling ocean acetone concentration (dashed blue line), changing the reactivity factor for dry deposition (dashed brown line), and doubling biomass burning emissions (dashed orange line). Field measurements from Solberg et al., (1996) are shown as solid black dots. The modeled estimates are overlaid with monthly (solid circles) or seasonal (solid lines) field measurements, as found in the literature (de Gouw et al., 2004; Dolgorouky et al., 2012; Galbally et al., 2007; Guérette et al., 2019; Hu et al., 2013; Huang et al., 2020; Langford et al., 2010; Legrand et al., 2012; Li et al., 2019; Read et al., 2012; Schade and Goldstein, 2006).

ATom comparisons

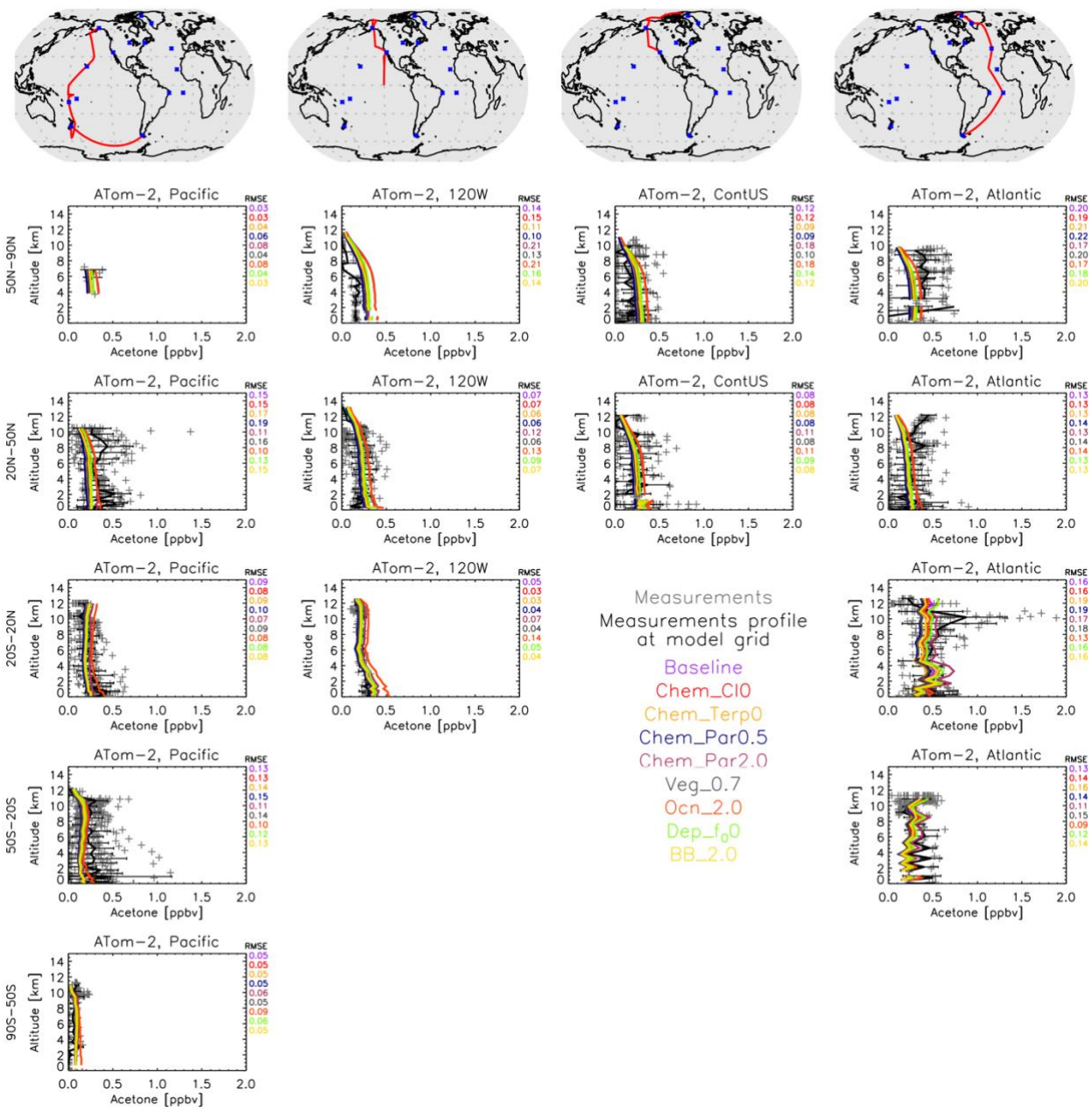

Figure S19. Similar to Figure S3, except a comparison between the GISS ModelE2.1 sensitivity simulations and the ATom-2 aircraft measurements (January-February 2017). Individual data points are shown with dark grey symbols, and their average values are shown in black, with error bars representing the one-sigma range of the averages. The root mean square error (RMSE) of each simulation is noted at the top right of each subplot. Note that all sensitivities are to be compared against the Baseline simulation.

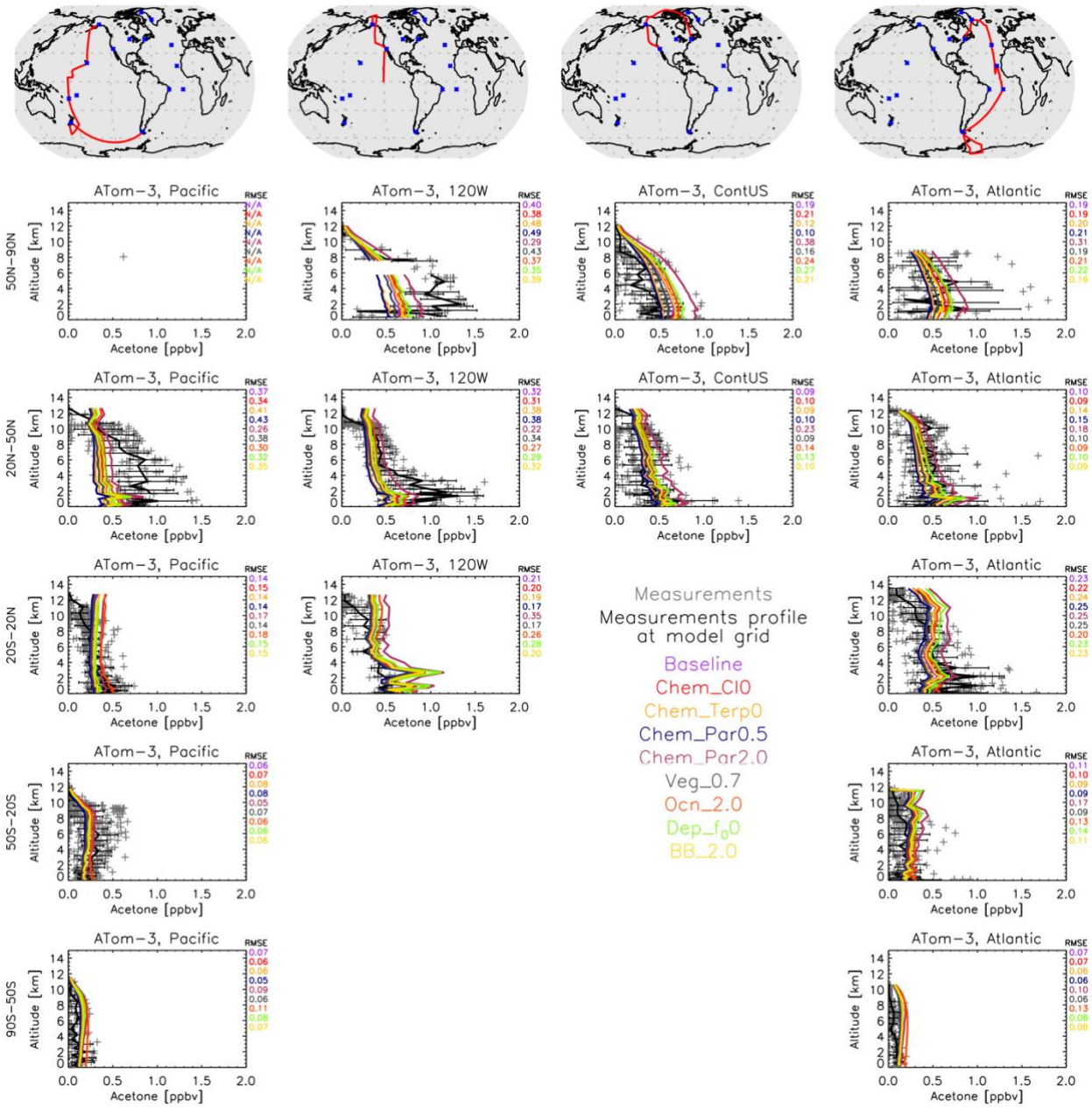

137

138 **Figure S20.** Similar to Figure S19, except for the ATom-3 field measurements (September-October 2017).

139

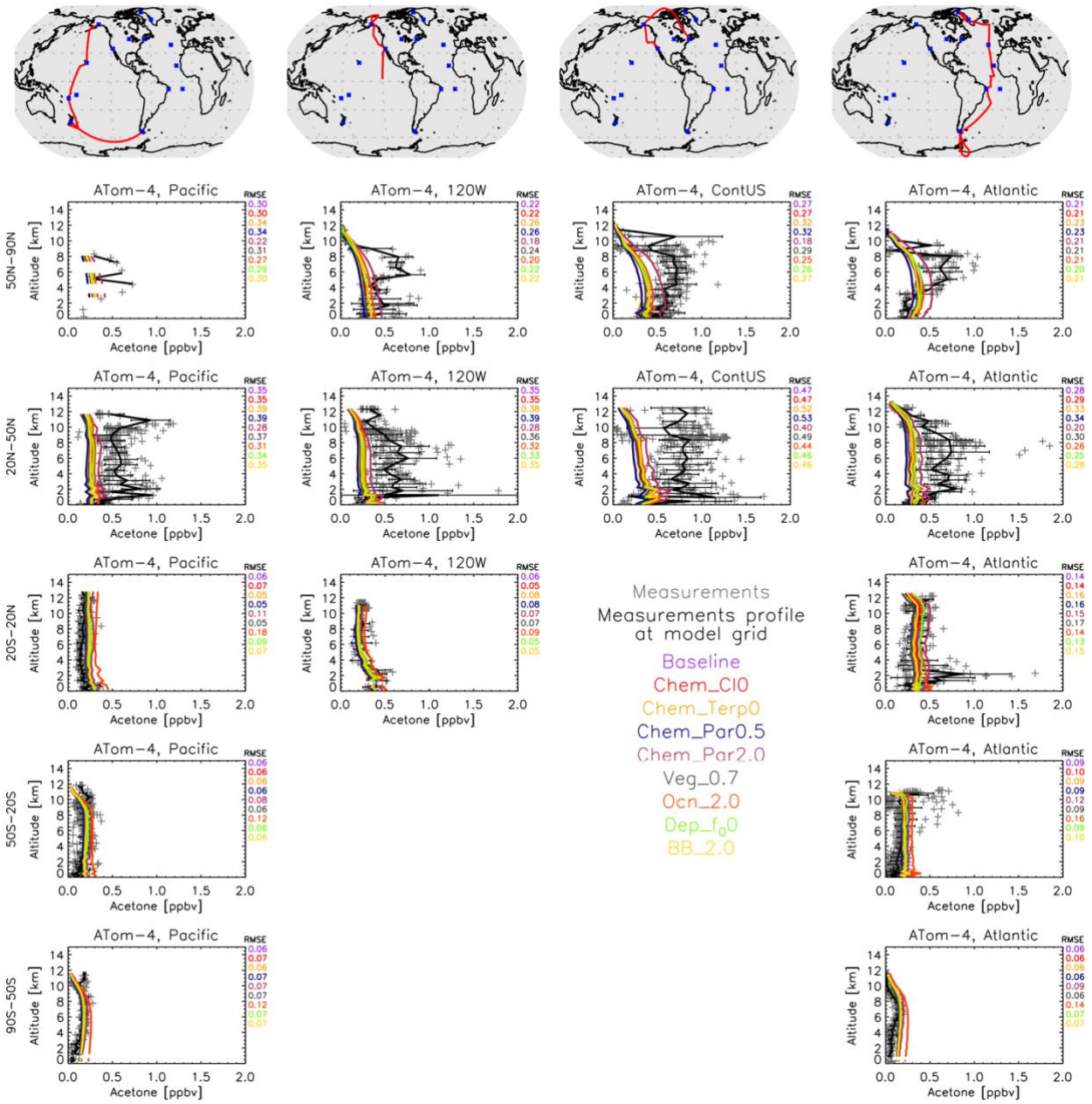

Figure S21. Similar to Figure S19, except for the ATom-4 field measurements (April-May 2018).

References

Arnold, S. R., Chipperfield, M. P., and Blitz, M. A.: A three-dimensional model study of the effect of new temperature-dependent quantum yields for acetone photolysis, J. Geophys. Res. Atmospheres, 110, https://doi.org/10.1029/2005JD005998, 2005.

Beale, R., Dixon, J. L., Arnold, S. R., Liss, P. S., and Nightingale, P. D.: Methanol, acetaldehyde, and acetone in the surface waters of the Atlantic Ocean, J. Geophys. Res. Oceans, 118, 5412–5425, https://doi.org/10.1002/jgrc.20322, 2013.

Brewer, J. F., Bishop, M., Kelp, M., Keller, C. A., Ravishankara, A. R., and Fischer, E. V.: A sensitivity analysis of key natural factors in the modeled global acetone budget, J. Geophys. Res. Atmospheres, 122, 2043–2058, https://doi.org/10.1002/2016JD025935, 2017.

Dolgorouky, C., Gros, V., Sarda-Esteve, R., Sinha, V., Williams, J., Marchand, N., Sauvage, S., Poulain, L., Sciare, J., and Bonsang, B.: Total OH reactivity measurements in Paris during the 2010 MEGAPOLI winter campaign, Atmospheric Chem. Phys., 12, 9593–9612, https://doi.org/10.5194/acp-12-9593-2012, 2012.

Dufour, G., Szopa, S., Harrison, J. J., Boone, C. D., and Bernath, P. F.: Seasonal variations of acetone in the upper troposphere–lower stratosphere of the northern midlatitudes as observed by ACE-FTS, J. Mol. Spectrosc., 323, 67–77, https://doi.org/10.1016/j.jms.2016.02.006, 2016.

Elias, T., Szopa, S., Zahn, A., Schuck, T., Brenninkmeijer, C., Sprung, D., and Slemr, F.: Acetone variability in the upper troposphere: analysis of CARIBIC observations and LMDz-INCA chemistry-climate model simulations, Atmospheric Chem. Phys., 11, 8053–8074, https://doi.org/10.5194/acp-11-8053-2011, 2011.

Fischbeck, G., Bönisch, H., Neumaier, M., Brenninkmeijer, C. A. M., Orphal, J., Brito, J., Becker, J., Sprung, D., van Velthoven, P. F. J., and Zahn, A.: Acetone–CO enhancement ratios in the upper troposphere based on 7 years of CARIBIC data: new insights and estimates of regional acetone fluxes, Atmospheric Chem. Phys., 17, 1985–2008, https://doi.org/10.5194/acp-17-1985-2017, 2017.

Fischer, E. V., Jacob, D. J., Millet, D. B., Yantosca, R. M., and Mao, J.: The role of the ocean in the global atmospheric budget of acetone, Geophys. Res. Lett., 39, https://doi.org/10.1029/2011GL050086, 2012.

Folberth, G. A., Hauglustaine, D. A., Lathière, J., and Brocheton, F.: Interactive chemistry in the Laboratoire de Météorologie Dynamique general circulation model: model description and impact analysis of biogenic hydrocarbons on tropospheric chemistry, Atmospheric Chem. Phys., 6, 2273–2319, https://doi.org/10.5194/acp-6-2273-2006, 2006.

Galbally, I., Lawson, S. J., Bentley, S., Gillett, R., Meyer, M., and Goldstein, A.: Volatile organic compounds in marine air at Cape Grim, Australia, Environ. Chem. - Env. CHEM, 4, https://doi.org/10.1071/EN07024, 2007.

de Gouw, J., Warneke, C., Holzinger, R., Klüpfel, T., and Williams, J.: Inter-comparison between airborne measurements of methanol, acetonitrile and acetone using two differently configured PTR-MS instruments, Int. J. Mass Spectrom., 239, 129–137, https://doi.org/10.1016/j.ijms.2004.07.025, 2004.

Guenther, A. B., Jiang, X., Heald, C. L., Sakulyanontvittaya, T., Duhl, T., Emmons, L. K., and Wang, X.: The Model of Emissions of Gases and Aerosols from Nature version 2.1 (MEGAN2.1): an extended and updated framework for modeling biogenic emissions, Geosci. Model Dev., 5, 1471–1492, https://doi.org/10.5194/gmd-5-1471-2012, 2012.

Guérette, É.-A., Paton-Walsh, C., Galbally, I., Molloy, S., Lawson, S., Kubistin, D., Buchholz, R., Griffith, D. W. T., Langenfelds, R. L., Krummel, P. B., Loh, Z., Chambers, S., Griffiths, A., Keywood, M., Selleck, P., Dominick, D., Humphries, R., and Wilson, S. R.: Composition of Clean Marine Air and Biogenic Influences on VOCs during the MUMBA Campaign, Atmosphere, 10, 383, https://doi.org/10.3390/atmos10070383, 2019.

Hu, L., Millet, D. B., Kim, S. Y., Wells, K. C., Griffis, T. J., Fischer, E. V., Helmig, D., Hueber, J., and Curtis, A. J.: North American acetone sources determined from tall tower measurements and inverse modeling, Atmospheric Chem. Phys., 13, 3379–3392, https://doi.org/10.5194/acp-13-3379-2013, 2013.

Huang, X.-F., Zhang, B., Xia, S.-Y., Han, Y., Wang, C., Yu, G.-H., and Feng, N.: Sources of oxygenated volatile organic compounds (OVOCs) in urban atmospheres in North and South China, Environ. Pollut., 261, 114152, https://doi.org/10.1016/j.envpol.2020.114152, 2020.

Jacob, D. J., Field, B. D., Jin, E. M., Bey, I., Li, Q., Logan, J. A., Yantosca, R. M., and Singh, H. B.: Atmospheric budget of acetone, J. Geophys. Res. Atmospheres, 107, ACH 5-1-ACH 5-17, https://doi.org/10.1029/2001JD000694, 2002.

Khan, M. A. H., Cooke, M. C., Utembe, S. R., Archibald, A. T., Maxwell, P., Morris, W. C., Xiao, P., Derwent, R. G., Jenkin, M. E., Percival, C. J., Walsh, R. C., Young, T. D. S., Simmonds, P. G., Nickless, G., O'Doherty, S., and Shallcross, D. E.: A study of global atmospheric budget and distribution of acetone using global atmospheric model STOCHEM-CRI, Atmos. Environ., 112, 269–277, https://doi.org/10.1016/j.atmosenv.2015.04.056, 2015.

Langford, B., Nemitz, E., House, E., Phillips, G. J., Famulari, D., Davison, B., Hopkins, J. R., Lewis, A. C., and Hewitt, C. N.: Fluxes and concentrations of volatile organic compounds above central London, UK, Atmospheric Chem. Phys., 10, 627–645, https://doi.org/10.5194/acp-10-627-2010, 2010.

Legrand, M., Gros, V., Preunkert, S., Sarda-Estève, R., Thierry, A.-M., Pépy, G., and Jourdain, B.: A reassessment of the budget of formic and acetic acids in the boundary layer at Dumont d'Urville (coastal Antarctica): The role of penguin emissions on the budget of several oxygenated volatile organic compounds, J. Geophys. Res. Atmospheres, 117, https://doi.org/10.1029/2011JD017102, 2012.

Li, K., Li, J., Tong, S., Wang, W., Huang, R.-J., and Ge, M.: Characteristics of wintertime VOCs in suburban and urban Beijing: concentrations, emission ratios, and festival effects, Atmospheric Chem. Phys., 19, 8021–8036, https://doi.org/10.5194/acp-19-8021-2019, 2019.

Marandino, C., Bruyn, W. J., Miller, S. D., Prather, M., and Saltzman, E.: Correction to "'Oceanic uptake and the global atmospheric acetone budget,'" https://doi.org/10.1029/2006GL028225, 2006.

Read, K. A., Carpenter, L. J., Arnold, S. R., Beale, R., Nightingale, P. D., Hopkins, J. R., Lewis, A. C., Lee, J. D., Mendes, L., and Pickering, S. J.: Multiannual Observations of Acetone, Methanol, and Acetaldehyde in Remote Tropical Atlantic Air: Implications for Atmospheric OVOC Budgets and Oxidative Capacity, Environ. Sci. Technol., 46, 11028–11039, https://doi.org/10.1021/es302082p, 2012.

Schade, G. W. and Goldstein, A. H.: Seasonal measurements of acetone and methanol: Abundances and implications for atmospheric budgets, Glob. Biogeochem. Cycles, 20, https://doi.org/10.1029/2005GB002566, 2006.

Singh, H., Chen, Y., Tabazadeh, A., Fukui, Y., Bey, I., Yantosca, R., Jacob, D., Arnold, F., Wohlfrom, K., Atlas, E., Flocke, F., Blake, D., Blake, N., Heikes, B., Snow, J., Talbot, R., Gregory, G., Sachse, G., Vay, S., and Kondo, Y.: Distribution and fate of selected oxygenated organic species in the troposphere and lower stratosphere over the Atlantic, J. Geophys. Res. Atmospheres, 105, 3795–3805, https://doi.org/10.1029/1999JD900779, 2000.

Singh, H. B., Salas, L. J., Chatfield, R. B., Czech, E., Fried, A., Walega, J., Evans, M. J., Field, B. D., Jacob, D. J., Blake, D., Heikes, B., Talbot, R., Sachse, G., Crawford, J. H., Avery, M. A., Sandholm, S., and Fuelberg, H.: Analysis of the atmospheric distribution, sources, and sinks of oxygenated volatile organic chemicals based on measurements over the Pacific during TRACE-P, J. Geophys. Res. Atmospheres, 109, https://doi.org/10.1029/2003JD003883, 2004.

Solberg, S., Dye, C., Schmidbauer, N., Herzog, A., and Gehrig, R.: Carbonyls and nonmethane hydrocarbons at rural European sites from the mediterranean to the arctic, J. Atmospheric Chem., 25, 33–66, https://doi.org/10.1007/BF00053285, 1996.

Wang, S., Apel, E. C., Schwantes, R. H., Bates, K. H., Jacob, D. J., Fischer, E. V., Hornbrook, R. S., Hills, A. J., Emmons, L. K., Pan, L. L., Honomichl, S., Tilmes, S., Lamarque, J.-F., Yang, M., Marandino, C. A., Saltzman, E. S., Bruyn, W. de, Kameyama, S., Tanimoto, H., Omori, Y., Hall, S. R., Ullmann, K., Ryerson, T. B., Thompson, C. R., Peischl, J., Daube, B. C., Commane, R., McKain, K., Sweeney, C., Thames, A. B., Miller, D. O., Brune, W. H., Diskin, G. S., DiGangi, J. P., and Wofsy, S. C.: Global Atmospheric Budget of Acetone: Air-Sea Exchange and the Contribution to Hydroxyl Radicals, J. Geophys. Res. Atmospheres, 125, e2020JD032553, https://doi.org/10.1029/2020JD032553, 2020.

Weimer, M., Schröter, J., Eckstein, J., Deetz, K., Neumaier, M., Fischbeck, G., Hu, L., Millet, D. B., Rieger, D., Vogel, H., Vogel, B., Reddmann, T., Kirner, O., Ruhnke, R., and Braesicke, P.: An emission module for ICON-ART 2.0: implementation and simulations of acetone, Geosci. Model Dev., 10, 2471–2494, https://doi.org/10.5194/gmd-10-2471-2017, 2017.